Growth of regular-shaped β-Ga$_2$O$_3$ nanorods by Ni^{2+}-ion-catalyzed chemical vapor deposition

Yuefeng Zhao · Shulian Liu · Yiqian Wang ·
Feng Shi · Zongjuan Zang

Abstract Regular-shaped monoclinic β-Ga$_2$O$_3$ nanorods with square cross-sections were successfully synthesized and characterized by Ni^{2+}-ion-catalyzed chemical vapor deposition method using CaF$_2$ as a dispersant. The composition, crystal structure, morphology, and optical property were characterized in detail. X-ray diffraction data indicate that the product was a single monoclinic β-Ga$_2$O$_3$ phase with high purity. The regular-shaped nanorods had square cross-sections and an approximate size of 250 nm in diameter and 500–1,000 nm in length. A broad and strong emission band that ranged from 300 to 650 nm was observed with three bands centered at approximately 405 (blue), 467 (dark blue), and 520 nm (green). The growth mechanism of β-Ga$_2$O$_3$ nanorods was consistent with the vapor–solid growth mechanism.

Shulian Liu and Yiqian Wang are joined first authors.

Y. Zhao · F. Shi (✉) · Z. Zang (✉)
College of Physics and Electronics, Shandong Normal
University, Jinan 250014, People's Republic of China
e-mail: sf751106@sina.com.cn

Z. Zang
e-mail: zangzongjuan@163.com

S. Liu
Shandong Cadre School of Quality and Technical Supervision,
Jinan 250014, People's Republic of China

Y. Wang
The Cultivation Base for State Key Laboratory, Qingdao
University, Qingdao 266071, People's Republic of China

1 Introduction

β-Ga$_2$O$_3$ has potential applications as a transparent conducting material in next-generation optoelectronic devices operating from the visible to ultraviolet spectrum because of its unique bulk properties (i.e., chemically and thermally stable compound with a wide band gap of 4.9 eV). In view of the superiority of nanostructures for future nanodevices, considerable efforts have been exerted to synthesize various β-Ga$_2$O$_3$ nanostructures, including nanowires, nanorods, nanoribbons, and nanobelts [1–5], using techniques such as carbothermal reduction [6], physical evaporation [7–10], microwave plasma reaction methods [4, 5], metal–organic chemical vapor deposition [11], and sol–gel methods [12]. However, most of these techniques require complicated equipment, extreme experimental conditions, or high cost.

We designed a simple, cost-effective, and convenient method to overcome these limitations. Ni-ion-catalyzed chemical vapor deposition (CVD) was used to synthesize β-Ga$_2$O$_3$ nanorods using CaF$_2$ as a dispersant. The composition, crystal structure, morphology, and photoluminescence (PL) property of the regular-shaped β-Ga$_2$O$_3$ nanorods with square cross-sections were analyzed in detail. In addition, the growth mechanism of the β-Ga$_2$O$_3$ nanorods was determined, which was consistent with the vapor–solid (VS) growth mechanism.

2 Experiment details

In our experiment, regular-shaped β-Ga$_2$O$_3$ nanorods with square cross-sections were grown in a hot-wall CVD apparatus using metallic Ga and an oxygen source. The raw materials used and their purities were as follows: metallic

Ga (99.99 %), NiCl$_2$•6H$_2$O crystal (99.9 %), CaF$_2$ (99.5 %), O$_2$ (99.999 %), and N$_2$ (99.999 %). The process was divided into three steps. The first step was the formation of NiCl$_2$-coated Si (111) substrates by dipping the substrates into 2 % NiCl$_2$ ethanol solution for 1 h and milling the Ga/CaF$_2$ mixture powders for 30 min in agate mortar at room temperature with a weight ratio of 1:2. The second step was the placement of the as-deposited substrates in the quartz boat approximately 10 mm away from the Ga/CaF$_2$ mixture powders (1.5 g). The last step involved the positioning of the quartz boat at the flat-temperature zone of the quartz tube furnace after increasing the furnace temperature to 1,050 °C and flushing of oxygen and moisture by N$_2$. Then, the furnace was annealed in O$_2$ atmosphere at a constant rate of 200 sccm for 30 min. The flowing N$_2$ gas was introduced into the quartz tube to flush out the residual O$_2$ for 10 min. Finally, the samples were obtained for characterization.

The composition, crystal structure, surface morphology, and light-emitting property of the samples were characterized using X-ray diffraction (XRD, Rigaku D/max-rB Cu Kα), Fourier transform infrared spectrophotometry (FTIR) with an Mg X-ray source (Bruker VERTEX-70), scanning electron microscopy (SEM, Hitachi S-570), high-resolution transmission electron microscopy (HRTEM, Hitachi 9000), and PL spectrophotometry (F-4500 fluorescence spectrophotometer).

3 Results and discussion

Figure 1 shows the XRD pattern of Ga2O3 nanorods annealed at 1,050 °C for 30 min, which was indexed to the monoclinic β-Ga2O3 (JCPDS:41-1103). Eight diffraction
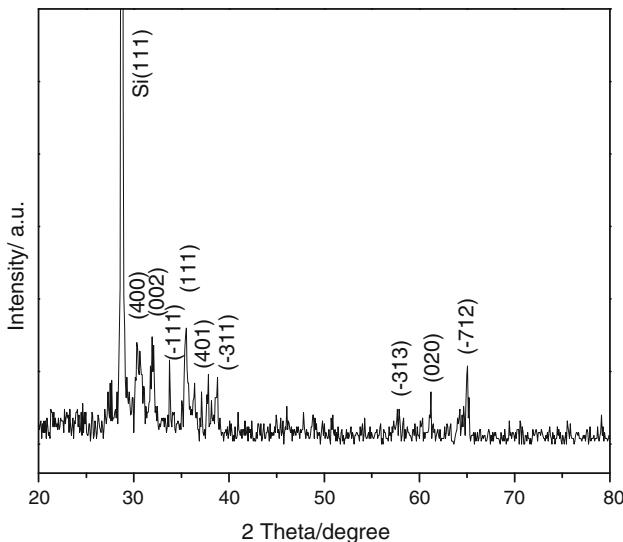
Fig. 1 XRD pattern of the sample
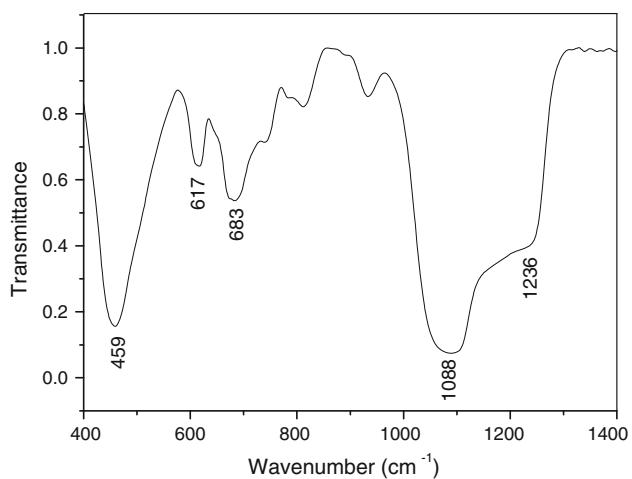
Fig. 2 FTIR spectra of the sample
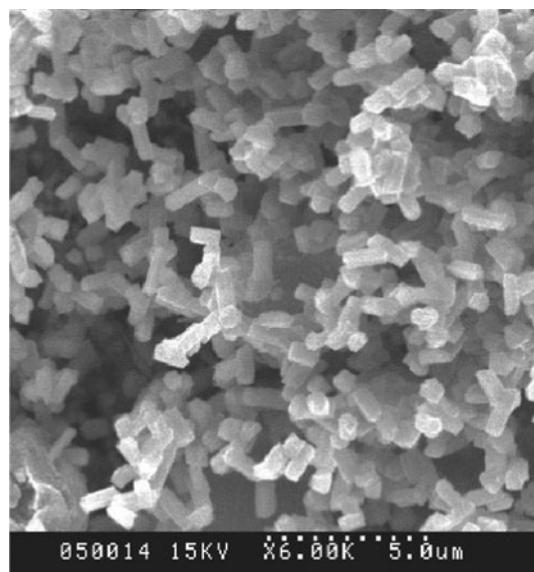
Fig. 3 SEM image of the sample

peaks were located at $2\theta = 30.32°$, 31.92°, 33.76°, 35.52°, 37.84°, 38.8°, 61.2°, and 65.04°, which corresponded to the (400), (002), (–111), (111), (401), (–311), (020), and (–712) planes, respectively. Strong diffraction peaks located at 28.72° were correlated with the Si (111) substrate. No diffraction peak was observed for impurities, which indicates that the product on the substrate was a single β-Ga$_2$O$_3$ phase with high purity.

FTIR was conducted to characterize the composition of the sample, as shown in Fig. 2. In the FTIR spectra, five well-defined prominent absorption bands located at 459, 617, 683, 1,088, and 1,236 cm^{-1} were observed. The strong bands at 459 and 683 cm^{-1} were due to Ga–O vibrations, and corresponded to the contraction vibrations of the octahedron GaO$_6$ and regular tetrahedron GaO$_4$, respectively, which were identical to that of bulk β-Ga$_2$O$_3$

Fig. 4 TEM, HRTEM, and SAED images of the sample
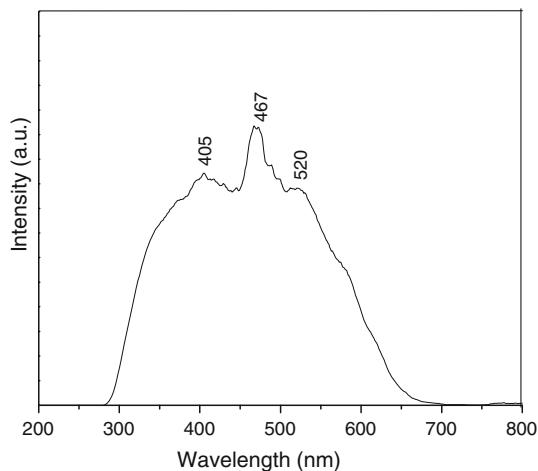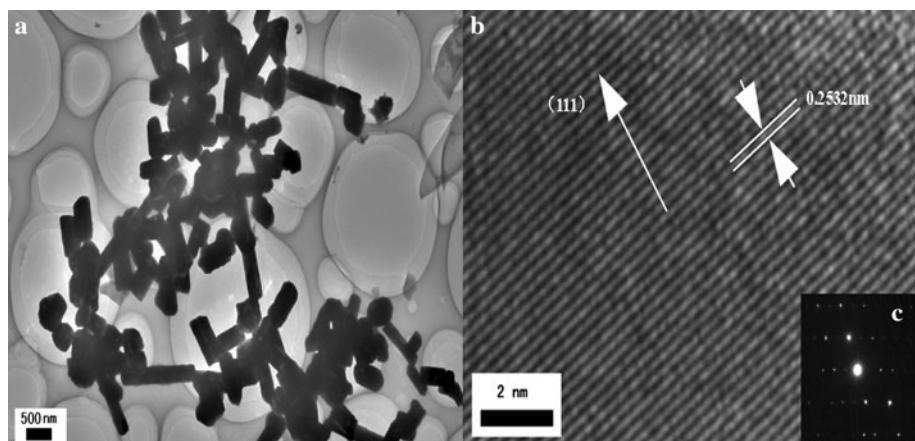
Fig. 5 Room-temperature PL spectra of β-Ga$_2$O$_3$ nanorods

[13]. The band centered at 617 cm^{-1} results from the local vibration of the substituted carbon in the Si crystal lattice [14]. The strong bands at 1,088 and 1,236 cm^{-1}, which correlated with the Si substrate, were due to the Si–O–Si asymmetric stretching vibration. The bands at 617, 1,088, and 1,236 cm^{-1} are related to the Si substrate [15, 16].

Fig. 3 shows the SEM image of the β-Ga2O3 nanorods annealed at 1,050 °C for 30 min. β-Ga2O3 nanorods were homogeneously distributed on the entire substrate surface with regular morphology, i.e., the surface of the nanorods were smooth and the boundaries were clear. Most of the nanorods were 250 nm in diameter and 500 to 1,000 nm in length. The cross-sections of the nanorods were square-shaped.

Fig. 4a shows that a typical individual nanorod was straight, had a smooth surface, a diameter of 250 nm, and an approximate length of 0.5 to 1.0 μm, which were consistent with Fig. 3. The Ga$_2$O$_3$ nanorod exhibited a solid rather than a hollow tubular structure. Figure 4b shows the HRTEM lattice image of the straight β-Ga$_2$O$_3$ nanorod. The spaced lattice fringe in the image indicates that the β-Ga$_2$O$_3$ nanorod was completely crystallized. The crystal plane spacing of the nanorod was approximately 0.2532 nm, which corresponded to the (111) crystal plane spacing of the monoclinic β-Ga$_2$O$_3$. The axis of the nanorod is shown in Fig. 5b. The SAED image (Fig. 4c) shows that the β-Ga$_2$O$_3$ sample was a single crystal, which was similar to the XRD results.

Figure 5 shows the room-temperature PL spectra of β-Ga$_2$O$_3$ nanorods excited at 250 nm. A broad and strong emission band that ranged from 300 nm to 650 nm was observed, and three bands were centered at approximately 405 (blue), 467 (dark blue), and 520 nm (green). This result indicates the existence of blue and green emissions. Excited nanorods emitted greater energy because of the larger surface area. Thus, the emission band had strong intensity with broad range. The green and blue emission peaks were attributed to the recombination of an electron on a donor because of the oxygen vacancy (V_O) and a hole on an acceptor because of gallium vacancy (V_{Ga}) or the gallium-oxygen vacancy pair (V_{Ga}–V_O) [17, 18]. Therefore [18, 19], the blue emission peak (405 nm) excited with the photon energy slightly below the band gap of β-Ga$_2$O$_3$ was considered as the recombination of the donor band (V_O) close to the valence band, and the acceptor band consisted of the gallium-oxygen vacancy pair (V_{Ga}–V_O). The blue and green emission peaks centered at 467 and 520 nm by Gaussian fitting were attributed to the recombination of an electron and hole that originated from donors because of oxygen vacancies (V_O) and acceptors because of gallium vacancy (V_{Ga}) or gallium-oxygen vacancy pairs (V_{Ga}–V_O) [19, 20]. These donor–acceptor pairs can form trapped excitons, which result in blue-green emission, according to the following process: $(V_O, V_{Ga})^{\times} + V_O^{\times} \rightarrow (V_O, V_{Ga})' + V_O + h\nu$ [20].

The formation mechanism of the β-Ga$_2$O$_3$ nanorods can be explained by the VS growth mechanism. Ni^{2+} ions have an important function during β-Ga$_2$O$_3$ crystal growth, and are catalysts for Ga$_2$O$_3$ embryos. An increase in Ni^{2+} ions

can change the energy distribution on the substrate surface, i.e., a large quantity of defect energies can be found with more broken bonds clustered on the sites where Ni^{2+} ions are distributed [21]. CaF_2, an important dispersant, increased the vaporization of metallic Ga at 1,050 °C during the reaction process, and facilitated the formation of β-Ga_2O_3 nanorods. Metallic Ga melted into small droplets, which were transported into the Ni^{2+}-ion-coated-substrate. Dissociative gaseous-state Ga and O atoms were absorbed by the broken bonds of the Ni^{2+} ions, and these atoms formed nucleation points. Free Ga and O atoms continued to spread and grow along the preferred orientation, which resulted in the formation of β-Ga_2O_3 nanorods. Ni^{2+} had an important function as a catalyst during the formation of β-Ga_2O_3 nanorods. CaF_2, an important dispersant, increased the vaporization of metallic Ga at 1,050 °C and facilitated the formation of β-Ga_2O_3 nanorods.

4 Conclusion

The regular-shaped β-Ga_2O_3 nanorods with square cross-sections were successfully obtained through a simple, cost-effective, and convenient catalyzed CVD method using CaF_2 as a dispersant and Ni^{2+} ions as catalysts. The composition, crystal structure, morphology, and PL property of the β-Ga_2O_3 nanorods were analyzed in detail. XRD showed that the sample was a single monoclinic β-Ga_2O_3 phase with high purity. The regular-shaped nanorods had square cross-sections and an approximate size of 250 nm in diameter and 500–1,000 nm in length. A broad and strong emission band ranging from 300 to 650 nm, which was attributed to a larger surface area of nanorods, was observed with three bands at approximately 405 (blue), 467 (dark blue), and 520 nm (green). Finally, the growth mechanism of the β-Ga_2O_3 nanorods was determined, which was consistent with the VS growth mechanism.

References

1. B. Das, S. Acharya, J Nanosci Nanotechnol **12**, 6258 (2012)
2. L.D. Tang, B. Wang, H.L. Du, J.Z. Wang, J Nanosci Nanotechnol **12**, 6385 (2012)
3. Y. Jang, J. Park, Y. Kim Pak, J. Jungho Pak, J Nanosci Nanotechnol **12**, 5173 (2012)
4. L.G. Gai, H.H. Jiang, Y. Tian, D.L. Cui, Q.L. Wang, Nanotechnology **17**, 5858–5861 (2006)
5. D.G. Yin, B.H. Liu, L. Zhang, M.H. Wu, J Biomed Nanotechnol **8**, 458 (2012)
6. L.D. Tang, B. Wang, H.L. Du, J.Z. Wang, J Nanosci Nanotechnol **12**, 6385 (2012)
7. A. Babu, K. Jeyasubramanian, P. Gunasekaran, R. Murugesan, J Biomed Nanotechnol **8**, 43 (2012)
8. F.P. Navarro, M. Berger, S. Guillermet, V. Josserand, L. Guyon, E. Neumann, F. Vinet, I. Texier, J Biomed Nanotechnol **8**, 730 (2012)
9. Y. Nam, J. Park, Y.K. Pak, J.J. Pak, J Nanosci Nanotechnol **12**, 5547 (2012)
10. T. Xiong, Y.J. Li, F.G. Ni, F. Zhang, J Biomed Nanotechnol **8**, 74 (2012)
11. C.H. Liang, G.W. Meng, G.Z. Wang, Y.W. Wang, L.D. Zhang, Appl Phys Lett **78**, 3202 (2001)
12. R. Jalilian, M.M. Yazdanpanah, B.K. Pradhan, G.U. Sumanase-kera, Chem Phys Lett **426**, 393 (2006)
13. H.D. Xiao, H.Y. Pei, W.R. Hu, B. Bo, Y.B. Qiu, Mater Lett **64**, 2399 (2010)
14. J.Q. Hu, Q. Li, X.M. Meng, C.S. Lee, S.T. Lee, J Phys Chem **B106**, 9536 (2002)
15. X.C. Wu, W.H. Song, W.D. Huang, M.H. Pu, B. Zhao, Y.P. Sun, J.J. Du, Chem Phys Lett **328**, 5 (2000)
16. Y. Sun, T. Miyasato, J Appl Phys **84**, 6451 (1998)
17. K.W. Chang, J.J. Wu, Adv Mater **16**, 545 (2004)
18. L.C. Tien, W.T. Chen, C.H. Ho, J Am Ceram Soc **94**, 3117 (2011)
19. Y.J. Zhang, J.L. Yan, Q.S. Li, C.Q.L.Y. Zhang, W.F. Xie, Mater Sci Eng **B176**, 846 (2011)
20. P.C. Chang, Z.Y. Fan, W.Y. Tseng, A. Rajagopal, J.G. Lu, Appl Phys Lett **87**, 222102 (2005)
21. F. Shi, X.W. Feng, J Nanosci Nanotechnol **12**(11), 8481–8486 (2012)